

## Compression Measurements of Neon-Seeded Glass Microballoons Irradiated by CO<sub>2</sub>-Laser Light

Kenneth B. Mitchell, David B. vanHusteyn, Gene H. McCall, and Ping Lee  
*Los Alamos Scientific Laboratory, University of California, Los Alamos, New Mexico 87545*

and

Hans R. Griem  
*Department of Physics and Astronomy, University of Maryland, College Park, Maryland 20742*  
 (Received 31 July 1978)

Compression of DT-neon-seeded, glass microballoons has been observed in CO<sub>2</sub>-laser experiments at Los Alamos Scientific Laboratory. DT densities of the order of 20% of liquid density have been attained. Detailed comparisons of the neon densities determined from the measured neon source size and from the fit of observed spectra by Stark-broadening calculations have been made. The excellent agreement obtained with these methods indicates that the extrapolation of the microfield effects used in Stark-broadening calculations to high densities is reasonable.

The seeding of glass-microballoon targets filled with deuterium-tritium (DT) mixtures with neon has received considerable attention recently in the laser-fusion community, since the neon affords a method for measuring target compression.<sup>1-3</sup> Yaakobi *et al.*<sup>1</sup> irradiated neon-filled targets with a four-beam Nd:glass laser and observed Stark-broadened neon lines which indicate electron densities of  $7 \times 10^{22}/\text{cm}^2$ . Key *et al.*,<sup>2</sup> have reported observation of spatially and spectrally resolved Stark-broadened neon lines emitted from glass microballoons imploded by a two-beam Nd:glass laser. Electron densities of  $1.7 \times 10^{23}/\text{cm}^3$  have been obtained. In this Letter, we report investigations of spatially resolved Stark-broadened neon lines produced in the two-beam CO<sub>2</sub>-laser experiment at Los Alamos Scientific Laboratory (LASL). The interaction of 10- $\mu\text{m}$  light with a plasma is qualitatively different from that of 1- $\mu\text{m}$  radiation,<sup>4</sup> and it is, therefore, important to study the physics of implosions produced using long-wavelength light. Also, the only laser currently under construction which has the possibility of producing significant thermonuclear yield is a CO<sub>2</sub> laser,<sup>5</sup> and the CO<sub>2</sub> laser is the only known laser which has an efficiency high enough to be useful for eventual commercial application. In particular, a detailed comparison has been made between the compression as determined by measuring the neon core size and by fitting the observed line profiles with those expected from Stark broadening.<sup>6</sup>

The targets used in the experiment were 180- $\mu\text{m}$  (nominal) diameter glass microballoons with 1.1- $\mu\text{m}$  wall thickness filled with DT-neon mixtures at pressures ranging from 0.7 atm to 10 atm. The neon mass density in all cases was 0.9 mg/

cm<sup>3</sup> atm as opposed to the DT density of 0.225 mg/cm<sup>3</sup> atm; i.e., neon atoms constituted 10% of the total number of gas molecules. Since neon has a large effect on the thermal conductivity of the fuel region and on the implosion dynamics, an attempt was made to use the minimum amount required for detection of the spectral lines. The laser used in the experiments was the LASL two-beam CO<sub>2</sub> laser<sup>7</sup> which produces from 0.1 to 0.8 TW on target with a pulse length of 1.2 ns full width at half maximum (FWHM).

Space-resolved time-integrated spectra were taken with a flat thallium acid phthalate (TAP) crystal spectrograph with slits perpendicular to the dispersion direction. Frequently, two adjacent slits of widths 24 and 58  $\mu\text{m}$  were used to evaluate spectrograms with different spatial resolution on a single-shot basis. The spectrograph has a spatial magnification of  $3.05 \times$  over the instrument's range from 9.7 to 14.7  $\text{\AA}$ . Eight single-shot exposures were made on Kodak 2490 loaded in 16 mm strips in a cassette film transport. Film densities were converted to exposures (ergs per square centimeter) from x-ray film calibrations.<sup>8</sup>

Figure 1 shows a spatially resolved x-ray spectrogram from an 8.6-atm DT-neon-filled target. The slit width in this case was 65  $\mu\text{m}$ . The observed features include neon and sodium lines in first order and silicon lines in second order. The silicon and sodium He-like lines have a spatial extent of about 180  $\mu\text{m}$ , which is the diameter of the target. All of the neon lines appear in the center of the spectrogram and have a spatial extent of approximately 45  $\mu\text{m}$ . This result provides direct and unambiguous evidence of compression.

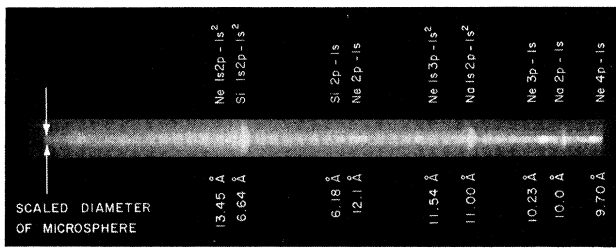


FIG. 1. Spatially resolved x-ray spectrogram from a glass microballoon target. The He-like silicon and sodium lines have a spatial extent of about 180  $\mu\text{m}$ , the diameter of the target. All of the neon lines in the center of the spectrogram have a spatial extent of 45  $\mu\text{m}$ .

These spatial differences can be seen more graphically in the microdensitometer scans shown in Fig. 2. The lower trace is a scan through the center of the spectrogram (i.e., through the core of the plasma). The upper trace is at the edge of the spectrogram and, therefore, scans the corona of the plasma. He-like lines of sodium and silicon dominate in the corona of the sources; H-like lines of silicon and neon are present only in the core. Furthermore, the continuum is observable only in the core.

Intensity ratios of silicon and neon lines indicate that the core is nearly 100 eV hotter than the corona. Analysis of neon line ratios yields core temperatures in the range of 350–400 eV when opacities of neon lines are taken into account.

The physical size of the compressed core was determined from spatial scans of lines perpendicular to the dispersion direction. The effect of the slit width on the size of the spatial image was evaluated experimentally from images produced with adjacent spectrograph slits. The density on film was converted to exposures for both lines and continuum. The line exposures were obtained by subtracting the exposure due to continuum that was present along side the spatial line image. The line exposure  $I(x)$ , is given by

$$I(x) = (2\delta)^{-1} \int_{x-\delta}^{x+\delta} S(x') dx', \quad (1)$$

where  $S(x)$  is the spatial intensity distribution from the source,  $\delta = \frac{1}{2}w(1 + M^{-1})$ ,  $w$  is the slit width,  $M$  is the magnification, and diffraction is neglected.

The source distribution,  $S(x)$ , can be deter-

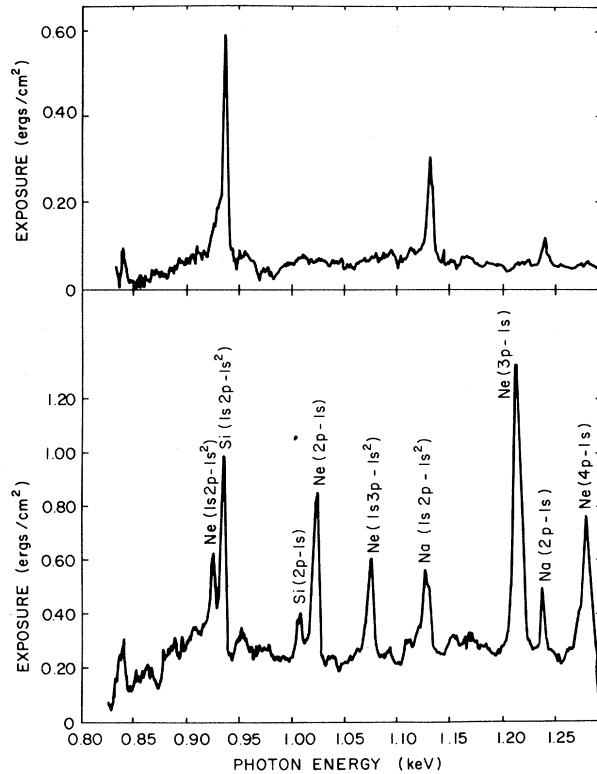


FIG. 2. Microdensitometer traces of the spatially resolved x-ray spectrogram (9-atm DT, 1-atm neon, 545 J, shot 0081). The upper trace gives a scan through the edge of the spectrogram, i.e., the corona of the plasma. The lower trace is a scan through the center of the spectrogram, i.e., the core of the plasma. Note the position dependence of various lines.

mined, in principle, by differentiating Eq. (1), but noise in the data makes this approach impractical. Instead, a least-squares fit of an assumed source function to the data using Eq. (1) directly was done. It was found that the fit was not sensitive to the length of a chord of a cylinder in the viewing direction. This function was perturbed by a polynomial to give a trial source distribution of the form

$$S(x) = \left[ 1 - \left( \frac{x}{R} \right)^2 \right]^{1/2} \sum_{i=0}^n C_i x^i. \quad (2)$$

Figure 3 shows the result of this procedure. The solid curve is the intensity distribution at the film in the spatial direction, the dashed curve is the source function  $S(x)$  from Eq. (2), and the

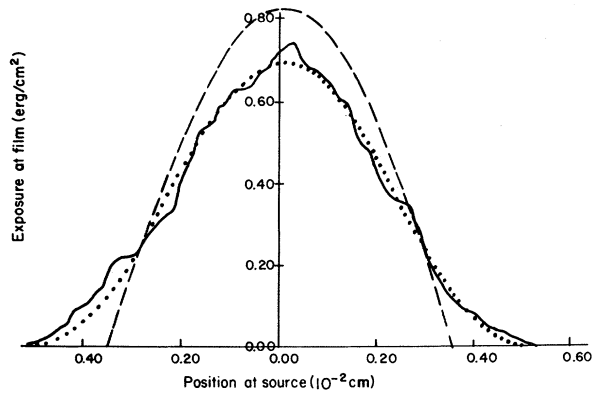


FIG. 3. Determination of the intensity distribution,  $S(x)$ , across the source for the neon  $L_\beta$  line. The solid curve is a microdensitometer scan along the spatially resolved direction of a neon  $L_\gamma$  line. The dotted curve is a reasonable estimate of  $S(x)$  and the dashed curve is the "best fit" to the experimental profile using Eq. (1). The source size in this case is  $64 \pm 2 \mu\text{m}$ .

dotted curve is the result of substituting Eq. (2) into Eq. (1). For this case the diameter of the compressed region is  $64 \pm 2 \mu\text{m}$ . The compressed diameters determined in this manner from spatial images of different slit widths agreed with each other to within 10% for the eight shots evaluated. As a result we believe that the volume compressions of a uniform source can be determined to about 30% using this technique.

Another significant feature of the spectra is that Stark broadening of neon lines is present. Here analysis of spectra taken with large slit widths (in the spatial direction) offer a distinct signal-to-noise advantage. Figure 4 shows a microdensitometer trace of a neon Lyman- $\beta$  ( $L_\beta$ ) line taken in the spectral direction. The dotted and dashed curves are "best fits" to the experimental line profile based on calculations of Griem, Blaha, and Kepple.<sup>5</sup> Doppler effect, finite source size, and crystal rocking angle have been folded into the Stark profile. The dotted curve is for the case where the opacity at line center  $\tau_{\text{max}} = 0$ , and the dashed curve corresponds to  $\tau_{\text{max}} = 1$ . It can be seen that both curves fit well at the wings and both imply an electron density of  $1.9 \times 10^{22}/\text{cm}^3$ ; the final DT density is  $1.0 \times 10^{22}/\text{cm}^3$ , which is about 20% of DT liquid density. A Stark profile fit of the  $L_\gamma$  line indicates a similar electron density, but the opacity at line center was only 0.3. With a temperature  $T_e \sim 350 \text{ eV}$ , the calculated densities of Ne X and Ne XI are found to be  $3.0 \times 10^{20}/\text{cm}^3$  and  $7.5 \times 10^{20}/\text{cm}^3$ , respec-

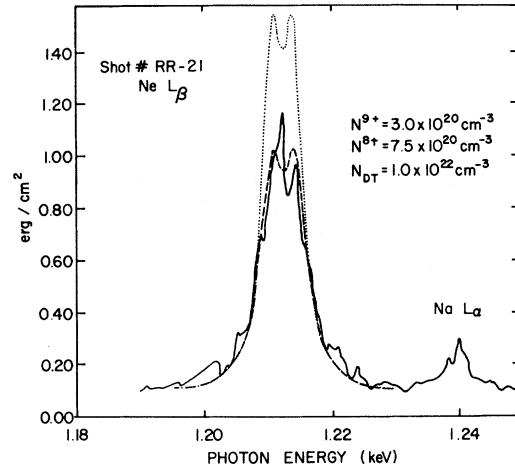


FIG. 4. Density determination: Fitting of a Stark profile (dashed and dotted curve) for  $N_e = 1.9 \times 10^{22}/\text{cm}^3$  to the experimental line profile (solid curve). The dotted curve is for the case where the optical depth at line center,  $\tau_{\text{max}}$ , is zero. The dashed curve is for the case  $\tau_{\text{max}} = 1$ .

tively. We note that the observed Stark width of  $21 \text{ m}\text{\AA}$  dominates the observed linewidth, while Doppler broadening, crystal rocking angle, and the effect of finite source size contribute only 2, 6, and  $5 \text{ m}\text{\AA}$ , respectively.

Self-consistent calculations of self-absorption<sup>9</sup> indicate that the opacities at line center ( $\tau_{\text{max}}$ ) are 30, 1, and 0.3 for  $L_\alpha$ ,  $L_\beta$ , and  $L_\gamma$ , respectively. The dominant broadening mechanism for the  $L_\alpha$  line is thus found to be self-absorption, while  $L_\beta$  and  $L_\gamma$  are nearly optically thin and broadened primarily by Stark effect.

In the Stark-broadening method of electron-density measurement, an accurate fit to the wings of a line is very important,<sup>6</sup> since for this region of the profile the theory is quite accurate. An estimated error of 25% or less due to noise and possible asymmetries in the actual lines usually exists in fitting the calculation to the experimental line profile.

Table I gives a comparison between the technique of source-size measurement and the Stark-broadening methods for three shots with different laser powers on target. The neon densities deduced from the source-size measurement agree very well with the Stark results for all three shots, which is a good indication that the extrapolation of the electric microfield effect used in Stark-broadening calculations to high densities ( $\sim 10^{22}/\text{cm}^3$ ) is reasonable. It is interesting to

TABLE I. Comparison of the source-size method vs the Stark-broadening calculations for measuring the compressed neon densities. Three shots of comparable fill pressure but different laser power are presented. Note that the volume compression is only slightly dependent on laser power on target. Neon source size was determined for the 24- $\mu\text{m}$  slit. The microsphere was 10% Ne by volume.

Shot No.	Target fill DT + Ne (atm)	Laser power ( $10^{11}$ W)	Initial diam. ( $\mu\text{m}$ )	Final diam. ( $\mu\text{m}$ )	Neon density, volume measurement ( $10^{20}$ $\text{cm}^{-3}$ )	Neon density, Stark ( $10^{20}$ $\text{cm}^{-3}$ )	Volume compression, Stark
RR-11	8	3.24	189	62	$3.2 \pm 1.3$	4.1	28
RR-21	8	4.52	185	50	$5.1 \pm 2$	6.8	50
RR-26	7	8.22	181	44	$5.5 \pm 2.4$	5.6	70

note that volume compression is slightly dependent on laser power. This agrees well with the exploding-pusher model,<sup>10</sup> which assumes that the fuel and the pusher are in thermal equilibrium.

The authors wish to express their appreciation to Robert Godwin of LASL for his extremely helpful comments on self-absorption of the lines and to Paul Kepple the Naval Research Laboratory for his calculations of the line profiles. We are also grateful to Paul Rockett, Damon Giovanielli, and Robert Godwin of LASL for their help in performing this research.

<sup>1</sup>B. Yaakobi, D. Steel, E. Thorsos, A. Hauer, and B. Perry, Phys. Rev. Lett. **39**, 1526 (1977).

<sup>2</sup>M. H. Key, R. G. Evans, D. J. Nichols, F. O'Neill, P. T. Rumsby, I. N. Ross, W. T. Toner, P. R. Williams, M. S. White, C. L. S. Lewis, J. G. Lunney, A. Moore, J. M. Ward, D. Brown, P. Carter, T. A. Hall, T. P. Hughes, P. Salter, E. Frabrikessi, A. Raven, J. Murdoch, and J. Kilkenney, Central Laser Facility, Rutherford Laboratory Report No. RL-77-122/B

(unpublished).

<sup>3</sup>D. S. Bailey, University of California Research Laboratory Report No. UCRL-79861, 1977 (unpublished).

<sup>4</sup>D. W. Forslund, J. M. Kindel, and K. Lee, Phys. Rev. Lett. **39**, 284 (1977).

<sup>5</sup>T. F. Stratton, F. P. Durham, J. Jansen, W. T. Leland, W. H. Reichelt, and V. L. Zeigler, in Proceedings of a Topical Meeting on Inertial Confinement Fusion, San Diego, California, 1978 (unpublished), Paper No. TU 7. Also see papers following.

<sup>6</sup>H. R. Griem, M. Blaha, and P. C. Kepple, Phys. A (to be published); see also P. C. Kepple and H. R. Griem, Naval Research Laboratory Memorandum Report No. 3634, 1978 (unpublished).

<sup>7</sup>J. V. Parker, M. J. Nutter, J. J. Hayden, and S. Singer, in Proceedings of a Conference on Laser and Electro-optical Systems, San Diego, California, 1976 (unpublished), Paper No. WG 2.

<sup>8</sup>For x-ray calibration of RAR 2490 see R. F. Benjamin, P. B. Lyons, and R. H. Day, Appl. Opt. **16**, 393 (1976).

<sup>9</sup>R. D. Cowan and G. H. Dieke, Rev. Mod. Phys. **20**, 518 (1948).

<sup>10</sup>D. V. Giovanielli and C. W. Cranfill, LASL Report No. LA-7218-MA, 1978 (unpublished).

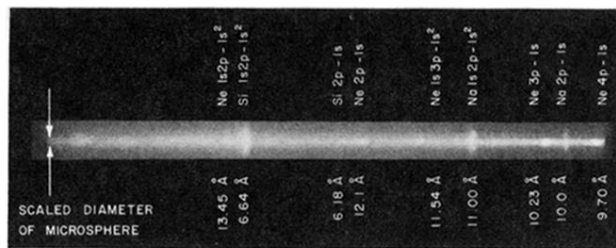


FIG. 1. Spatially resolved x-ray spectrogram from a glass microballoon target. The He-like silicon and sodium lines have a spatial extent of about  $180 \mu\text{m}$ , the diameter of the target. All of the neon lines in the center of the spectrogram have a spatial extent of  $45 \mu\text{m}$ .